

Decomposition and Sticking of Hydrocarbons in the Plasma Generator PSI-2

W. Bohmeyer^{a,b} A. Markin^c D. Naujoks^b B. Koch^{a,b} G. Krenz^a M. Baudach^a
G. Fussmann^{a,b}

^a*AG Plasmaphysik der Humboldt Universität, Newtonstr. 15, D-12489 Berlin, Germany*

^b*MPI für Plasmaphysik, EURATOM Ass., Garching, Germany*

^c*Institute of Physical Chemistry, Russian Academy of Sciences, Moscow, Russia*

Abstract

Hydrocarbons were injected into the plasma generator PSI II to study the formation of deposition layers. The experimental results are compared with those obtained from ERO-code modelling. Using available data of rate and sticking coefficients in the simulations the agreement is not satisfying. New experimental results point to a hydrocarbon decomposition considerably stronger than predicted. Furthermore the occurrence of very active particles, having sticking probabilities near to unity, have to be postulated in contrast to the assumptions inherent to earlier simulations.

Key words: C0100 Carbon, R0900 Re-deposition, T0100 Theory and Modelling

PSI keywords: Carbon, erosion, amorphous carbon, carbon deposition, ERO

PACS: 81.15-Z

1. Introduction

It is well known that fusion devices using carbon as wall material are endangered by long-term retention of tritium in the surface layers resulting from sticking of various hydrocarbon molecules. In fact, estimates show that the tritium inventory accumulated in ITER this way may easily pass the acceptable level[1].

In order to investigate the relevant processes involved in hydrocarbon disintegration/ transformation and sticking on the walls experiments have

been performed in the PSI-2 plasma generator. Earlier studies[2] had revealed large discrepancies between experiment and modelling. The latter was done by feeding into the ERO code the sticking coefficients as measured by C. Hopf et al. [3], valid for thermal energies (≈ 0.025 eV), and the atomic data package from the Janev/Reiter compilation[4].

Here we report on additional experiments allowing some simple estimation. In addition a new data set of calculated sticking coefficients[5] will be checked.

Email address: werner.bohmeyer@ipp.mpg.de (W. Bohmeyer^{a,b}).

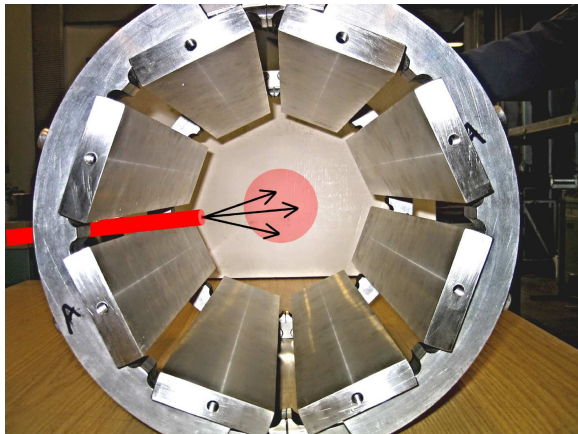


Figure 1. Eight tiles baring Si-collectors are arranged around the plasma column. Hydrocarbons are injected from the left hand side.

2. Experimental arrangement

The PSI-2, a stationary high current arc discharge, is used for deposition experiments, similar to those described in [2]. Well defined amounts of CH_4 or C_2H_4 are injected into the plasma through a nozzle at the plasma edge. Simultaneously the deposition pattern growing on the water cooled collector opposite to the nozzle is recorded in situ by optical measurements. In addition the blue light ($\lambda \approx 430 \text{ nm}$) associated with the emission band of the CH molecules is detected with good space resolution using both, a spectrometer equipped with 16 fibre channels and a CCD camera. In order to get 2D- space resolved information on the thickness of the growing a-CH layers the eight heavy stainless steel tiles shown in Fig. 1 (baring Si-wafers on their top surfaces) are arranged co-axial to the plasma beam, i.e. parallel to the magnetic field, in the near nozzle region. They cover a length of 420 mm. Minimizing the influence of erosion these deposition experiments are limited to 30 min. During this time the temperature increase of the tiles is less than 50 K. Furthermore, two quadrupole mass spectrometers (QMS) were used to analyse the gas: QMS I gives information about the gas composition in the target chamber whereas QMS II analyses the exhaust.

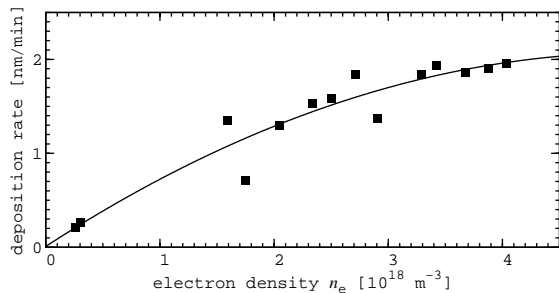


Figure 2. Deposition rate versus electron density measured for an injection of 0.5 sccm CH_4 into Ar-plasmas.

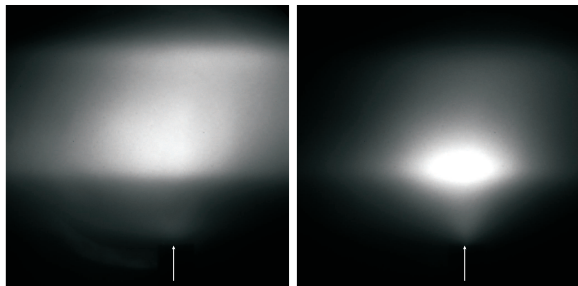


Figure 4. CH-emission patterns in a He discharge for low (left, $n_e = 5 \cdot 10^{17} \text{ m}^{-3}$) and high (right, $n_e = 3 \cdot 10^{18} \text{ m}^{-3}$) electron density. The position of the nozzle is indicated by the arrow.

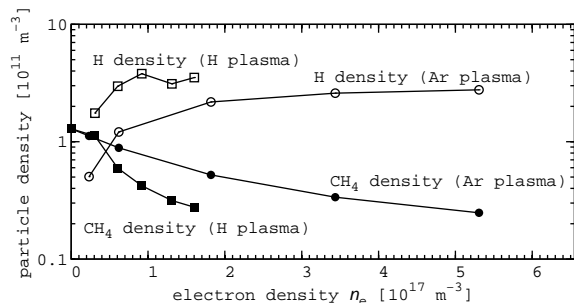


Figure 5. Particle density of H and CH_4 vs. n_e for methane injection into hydrogen (squares) and argon (circles) plasmas.

3. Experimental results

In contrast to discharges in hydrogen where erosion of the layers by H atoms plays an important role, this effect is completely suppressed in argon or helium discharges. For this reason these noble gases are better suited for a comparison with modelling since they allow to measure directly the proper

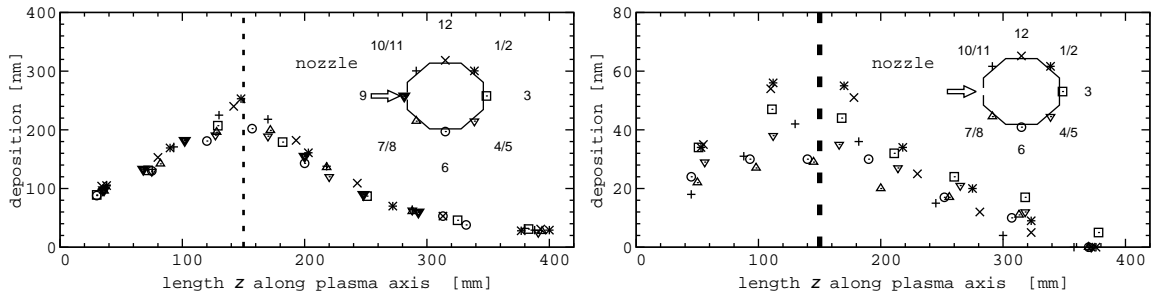


Figure 3. Deposition pattern from the 8 collectors for a H-plasma (left, $n_e = 4.0 \cdot 10^{17} \text{ m}^{-3}$) an Ar-plasma (right, $n_e = 2.3 \cdot 10^{18} \text{ m}^{-3}$).

deposition rates of the layers. Fig. 2 shows the corresponding rates when 0.5 sccm CH_4 is injected into an argon plasma with varying electron density. As to be seen there is initially a nearly linear rise with electron density but at finally saturation sets in. This behaviour can be understood in terms of an increasing influence of ionization of the injected hydrocarbons immediately behind the nozzle leading to a rapid loss of the particles along the magnetic field lines. The maximum deposition rate is found to $3.8 \text{ nm}/(\text{sccm} \cdot \text{min})$. When switching off the methane flow the film thickness stays constant indicating that in fact no erosion takes place.

In Fig. 3 two examples for local deposition patterns are shown. They are obtained from measuring the thickness of the layers on the eight tiles already mentioned. In the figures the thickness is plotted as a function of the length in the axial direction (z-coordinate) with the tile number (different symbols, representing the azimuthal angle θ) as a parameter. In the first case (Fig. 3, left) methane was blown into a hydrogen plasma ($n_e = 4 \cdot 10^{17} \text{ m}^{-3}$). Nearly 80 % of the injected carbon is found on the inner walls of a cylinder of 300 mm length near to the injection point. The deposition pattern is obviously symmetric with respect to the angle θ .

By contrast, a homogeneous film thickness of 21 to 25 nm, indicating a global decomposition of the injected hydrocarbons, is found in argon for nearly the same plasma density ($6 \cdot 10^{17} \text{ m}^{-3}$). For these conditions QMS shows that about 75 % of the injected carbon is retained in the target chamber and again 80 % of this amount is found on the inner walls. For getting a local deposition pattern in ar-

gon, as the one shown in Fig. 3(right), the electron density must be increased by about a factor of 5. There is hence a difference in decomposition for argon and hydrogen discharges to be noticed (for equal electron density) indicating that ionic processes, like charge exchange, are involved.

There is a general agreement that the decomposition of injected CH_4 to CH proceeds in a number of steps[4]. The decomposition region can be visualized by recording the CH band emission by means of the CD camera equipped with a narrow interference filter. In Fig. 4 such CH emission patterns are shown for helium discharges at two different electron densities. For low electron densities (global decomposition, Fig. 4 left) the emission is rather homogeneous whereas it is concentrated around the nozzle to a volume of $\leq 4 \text{ cm}$ in diameter at higher electron densities (local decomposition, Fig. 4 right).

The influence of the electron density on the equilibrium particle density of the injected hydrocarbon can be seen from the QMS data presented in Fig. 5. The figure shows the concentrations of H and CH_4 in hydrogen and argon discharges as a function of n_e . Already for electron densities as small as $n_e \approx 10^{17} \text{ m}^{-3}$ a noticeable decomposition is to be inferred from the decaying methane signal (showing a $1/n_e$ dependence). It can also be seen that the decomposition is more pronounced in hydrogen than in argon plasmas, possibly indicating that CX-processes are involved

4. ERO Modelling

The transport of the injected gas molecules (CH_4) has been analyzed using the 3-D Monte Carlo code ERO[5] which has been adapted to the geometry of the plasma generator PSI-2. The measured profiles of the plasma parameters T_e and n_e are included in the calculations. The motion of the molecules inside the nozzle with an inner diameter of 1 mm has been followed with ERO in the molecular flow regime via consecutive adsorption-desorption cycles using the cosine law to describe the angular distribution of the desorbing particles. In order to improve the agreement with experimental results[6] the zone of molecular flow regime was restricted to a length of 3.7 mm at the end of the nozzle.

By crossing the plasma column the injected methane molecules are ionised and dissociated resulting in a broad spectrum of various hydrocarbon species including H, H_2 and C. The processes considered in the simulations include electron-impact ionisation and dissociation, dissociative excitation, ionisation and recombination with electrons. Charge exchange reactions were not taken into account due to the lack of corresponding reaction rates.

In the simulations half a million particles are started with, thus good statistics is obtained. For the calculations presented here the Janev/Reiter[4] compilation of reaction rate coefficients together with the energy dependence of each individual reaction has been used. The observed fast decomposition close to the position of injection indicates that the reactions rates are too small - at least for electron temperatures in the range of a few eV. Therefore a constant factor has been applied for all reaction rates in the simulations.

The deposition on the collector plate (diameter 0.3 m) is mainly influenced by the assumed sticking model. Up to now, only sticking coefficients for thermal energies are available. These values were already used in previous studies[7] but resulted in much lower deposition rates as observed in the experiments. Recently, Molecular Dynamics (MD) simulations of the sticking process of energetic hydrocarbons indicated that the energy de-

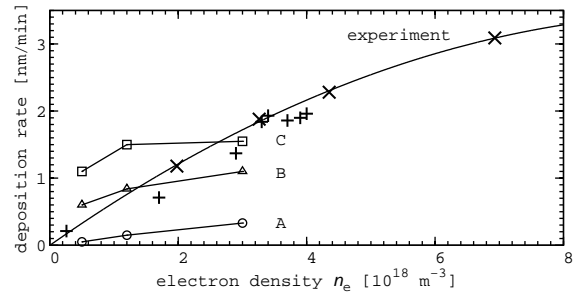


Figure 6. Deposition rate vs. electron density for a He (x) and an Ar (+) discharge. The results of modelling are included for He: A(circles): atomic data according[4], B(triangles): atomic data multiplied by a factor of 10, C(squares): as B and sticking coefficients according[9]

pendence of the sticking coefficients ($s = f(E)$) must be taken into account[8]. Detailed MD simulations have been performed meanwhile for a large number of hydrocarbons[9]. According to these calculations the sticking probability increases considerably with increasing energy of the incoming hydrocarbons reaching large values for energies of several electron volts. These new data have been incorporated in the ERO code presented in this paper.

In Fig. 6 we compare deposition rates determined by modelling and experiment. The original atomic data (A) predict a much smaller deposition rate than observed in the experiments. After multiplying the atomic data by a factor of 10 the simulations (B) match better the experimental data, especially for low electron densities (such an increase of the reaction rates can readily be obtained by shifting the temperature scale to lower values). A better agreement at higher electron densities appears attainable by including the energy dependence of the sticking coefficients (C).

5. Discussion and Summary

There are two essential experimental observations: (i) a rather high deposition rate of several nm/min even at very low plasma densities, and (ii) a bright and localized CH emission concentrating around the position where the methane is injected. The very short “reaction lengths”, along which CH_4 is transformed to CH, cannot be explained on

the basis of published data for the reaction rates. The latter have to be increased by about an order of magnitude to get rough agreement between experiment and simulation.

References:

References

- [1] G. Federici, C.H. Skinner, J.N. Brooks et al., Nuclear Fusion, vol. 41, pp. 1967-2137 (2001)
- [2] W. Bohmeyer, D. Naujoks, A. Markin, I. Arkhipov, B. Koch, D. Schröder, G. Fussmann, J. of Nucl. Mater. 337{339, 89 (2005).
- [3] C. Hopf, T. Schwarz-Selinger, W. Jacob, A. v. Keudell, J. Appl. Phys. 87 (2000) 2719
- [4] R. K. Janev, D. Reiter, Report Jül-3966, Institut für Plasmaphysik, Forschungszentrum, Jülich (2002)
- [5] Naujoks, D., Coster, D., Kastelewicz, H. and Schneider, R., J. Nucl. Mater., 266-269, 360 (1999).
- [6] G. Krenz, diploma thesis, Humboldt University, Berlin, 2005
- [7] Naujoks D., W. Bohmeyer, A. Markin, I. Arkhipov, P. Carl, B. Koch, H.-D. Reiner, D. Schröder, G. Fussmann, Physica Scripta 111, 80 (2004).
- [8] D. Alman, D. N. Ruzic, Physica Scripta, T111, 145 (2004).
- [9] A. Sharma, R. Schneider, U. Toussaint, K. Nordlund, Hydrocarbon Radicals Interaction With Amorphous Carbon Surfaces, this conference